JACS
JOURNAL OF THE AMERICAN CHEMICAL SOCIETY

Subscriber access provided by ISTANBUL TEKNIK UNIV

Article

Assessment of Water-Soluble □-Extended Squaraines as One- and Two-Photon Singlet Oxygen Photosensitizers: Design, Synthesis, and Characterization

Luca Beverina, Maurizio Crippa, Mirko Landenna, Riccardo Ruffo, Patrizio Salice, Fabio Silvestri, Silvia Versari, Alessandro Villa, Luca Ciaffoni, Elisabetta Collini, Camilla Ferrante, Silvia Bradamante, Claudio M. Mari, Renato Bozio, and Giorgio A. Pagani

J. Am. Chem. Soc., **2008**, 130 (6), 1894-1902 • DOI: 10.1021/ja075933a

Downloaded from http://pubs.acs.org on February 8, 2009

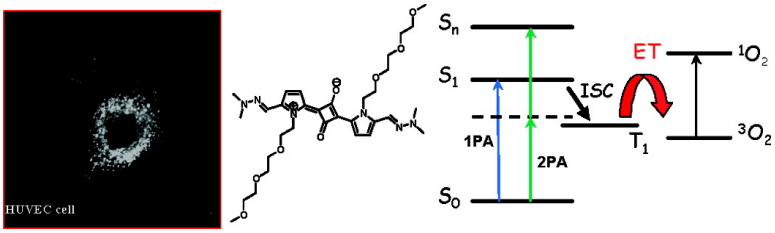

More About This Article

Additional resources and features associated with this article are available within the HTML version:

- Supporting Information
- Links to the 4 articles that cite this article, as of the time of this article download
- Access to high resolution figures
- Links to articles and content related to this article
- Copyright permission to reproduce figures and/or text from this article

View the Full Text HTML

ACS Publications
High quality. High impact.

Journal of the American Chemical Society is published by the American Chemical Society. 1155 Sixteenth Street N.W., Washington, DC 20036

J|A|C|S
ARTICLES
Published on Web 01/19/2008

Assessment of Water-Soluble π-Extended Squaraines as One- and Two-Photon Singlet Oxygen Photosensitizers: Design, Synthesis, and Characterization

Luca Beverina,*[,†] Maurizio Crippa,[†] Mirko Landenna,[†] Riccardo Ruffo,[†] Patrizio Salice,[†] Fabio Silvestri,[†] Silvia Versari,[‡] Alessandro Villa,[‡] Luca Ciaffoni,[§] Elisabetta Collini,[§] Camilla Ferrante,[§] Silvia Bradamante,[‡] Claudio M. Mari,[†] Renato Bozio,[§] and Giorgio A. Pagani*[,†]

Department of Materials Science and INSTM, University of Milano-Bicocca, via Cozzi 53, I-20125 Milano, Italy, Department of Chemistry and INSTM, University of Padova, via Marzolo 1, I-35131 Padova, Italy, and CNR-ISTM, Institute of Molecular Science and Technology, via Golgi 19, I-20133 Milan, Italy

Received August 7, 2007; Revised Manuscript Received December 4, 2007; E-mail: giorgio.pagani@mater.unimib.it; luca.beverina@mater.unimib.it

Abstract: Singlet oxygen sensitization by organic molecules is a topic of major interest in the development of both efficient photodynamic therapy (PDT) and aerobic oxidations under complete green chemistry conditions. We report on the design, synthesis, biology, and complete spectroscopic characterization (vis−NIR linear and two-photon absorption spectroscopy, singlet oxygen generation efficiencies for both one- and two-photon excitation, electrochemistry, intrinsic dark toxicity, cellular uptake, and subcellular localization) of three classes of innovative singlet oxygen sensitizers pertaining to the family of symmetric squaraine derivatives originating from π-excessive heterocycles. The main advantage of π-extended squaraine photosensitizers over the large number of other known photosensitizers is their exceedingly strong two-photon absorption enabling, together with sizable singlet oxygen sensitization capabilities, for their use at the clinical application relevant wavelength of 806 nm. We finally show encouraging results about the dark toxicity and cellular uptake capabilities of water-soluble squaraine photosensitizers, opening the way for clinical small animal PDT trials.

Introduction

Squaraines are the condensation products of electron-rich substrates and squaric acid. Because of the vast flexibility of their synthetic precursors, it is immediately clear that one important endowment of their composition is the extreme variety of their structure. Squaraines in fact have been extensively investigated since the mid 1960s[1] for a large number of technological applications including photoconductivity,[2] data storage,[3] light emitting field-effect transistors,[4] solar cells,[5] and nonlinear optics.[6] It has been recently shown that squaraines can also behave as very efficient two-photon absorbers,[7] fluorescent histological probes,[8] highly stable fluorescent near-IR dyes,[9] fluorescence patterning,[10] and possibly as second-generation photosensitizers for photodynamic therapy (PDT).[11]

PDT is an already employed, although yet nongeneral, nonsurgical protocol[12] for the treatment of a number of tumors including esophageal, bladder, lung, cervical, and skin cancer[13] and other non-neoplastic diseases such as age-related macular degeneration.[14] In a typical PDT treatment, a suitable dye, the photosensitizer,[15] is injected and selectively accumulated into

† University of Milano-Bicocca.
‡ Institute of Molecular Science and Technology.
§ University of Padova.

(1) For reviews of the synthesis of squaraines, see: (a) Schmidt, A. H. *Synthesis* **1980**, 961. (b) Sprenger, G. E.; Ziegenbein, W. *Angew. Chem., Int. Ed. Engl.* **1968**, *7*, 530. (c) Maahas, G.; Hegenberg, P. *Angew. Chem., Int. Ed. Engl.* **1966**, *5*, 888.
(2) (a) Law, K. Y. *J. Phys. Chem.* **1987**, *91*, 5184. (b) Law, K. Y. *Chem. Rev.* **1993**, *93*, 449. (c) Law, K. Y.; Bailey, F. C. *J. Org. Chem.* **1992**, *57*, 3278.
(3) (a) Emmelius, M.; Pawlowski, G.; Vollmann, H. W. *Angew. Chem.* **1989**, *101*, 1475. (b) Emmelius, M.; Pawlowski, G.; Vollmann, H. W. *Angew. Chem., Int. Ed. Engl.* **1989**, *28*, 1445.
(4) Smits, E. C. P.; Setayesh, S.; Anthopoulos, T. D.; Buechel, M.; Nijssen, W.; Coehoorn, R.; Blom, P. W. M.; de Boer, B.; de Leeuw, D. M. *Adv. Mater.* **2007**, *19*, 734.
(5) (a) Piechowski, A. P.; Bird, G. R.; Morel, D. L.; Stogryn, E. L. *J. Phys. Chem.* **1984**, *88*, 934. (b) Liang, K.; Law, K. Y.; Whitten, D. G. *J. Phys. Chem.* **1995**, *99*, 16704. (c) Burke, A.; Schmidt-Mende, L.; Ito, S.; Graetzel, M. *Chem. Commun.* **2007**, *3*, 234. (d) Yum, J.-H.; Walter, P.; Huber, S.; Rentsch, D.; Geiger, T.; Nuesch, F.; De Angelis, F.; Grätzel, M.; Nazeeruddin, M. K. *J. Am. Chem. Soc.* **2007**, *129*, 10320.
(6) (a) Chen, C.-T.; Marder, S. R.; Cheng, L. T. *J. Chem. Soc., Chem. Commun.* **1994**, 259. (b) Chen, C.-T.; Marder, S. R.; Cheng, L. T. *J. Am. Chem. Soc.* **1994**, *116*, 3117.
(7) Scherer, D.; Dörfler, R.; Feldner, A.; Vogtmann, T.; Schwoerer, M.; Lawrentz, U.; Grahn, W.; Lambert, C. *Chem. Phys.* **2002**, *279*, 179.
(8) Xiang, Z.; Nesterov, E. E.; Skoch, J.; Lin, T.; Hyman, B. T.; Swager, T. M.; Bacskai, B. J.; Reeves, S. A. *J. Histochem. Cytochem.* **2005**, *53*, 1511.
(9) (a) Arunkumar, E.; Forbes, C. C.; Noll, B. C.; Smith, B. D. *J. Am. Chem. Soc.* **2005**, *127*, 3288. (b) Johnson, J. R.; Fu, N.; Arunkumar, E.; Leevy, W. M.; Gammon, S. T.; Piwnica-Worms, D.; Smith, B. D. *Angew. Chem., Int. Ed.* **2007**, *46*, 5528.
(10) Liu, L.-H.; Nakatani, K.; Pansu, R.; Vachon, J.-J.; Tauc, P.; Ishow, E. *Adv. Mater.* **2007**, *19*, 433.
(11) (a) Ramaiah, D. A.; Joy, N.; Chandrasekar, N. V.; Eldho, S. D.; George, M. V. *Photochem. Photobiol.* **1997**, *65*, 783. (b) Ramaiah, D.; Eckert, I.; Arun, K. T.; Weidenfeller, L.; Epe, B. *Photochem. Photobiol.* **2002**, *76*, 672. (c) Ramaiah, D.; Eckert, I.; Arun, K. T.; Weidenfeller, L.; Epe, B. *Photochem. Photobiol.* **2004**, *79*, 99. (d) Santos, P. F.; Reis, L. V.; Almeida, P.; Serrano, J. P.; Oliveira, A. S.; Vieira Ferreira, L. F. *J. Photochem. Photobiol., A* **2004**, *163*, 267.

 10.1021/ja075933a CCC: $40.75 **© 2008 American Chemical Society**

the ill region. The selective accumulation can be either an intrinsic photosensitizer property, like in most of the hematoporphyrin-related[16] commercially available derivatives, or the consequence of the conjugation with a selective carrier.[17] The photosensitizer is a molecule possessing an accessible excited triplet state able to prompt, via excitation transfer, the formation of singlet oxygen ($^1O_2$), a very reactive, short living species.[18] The $^1O_2$ produced from ground state oxygen present at environmental levels in organic tissues readily results in cell death by either necrosis and/or apoptosis depending on the specific photosensitizer action and localization.[19] After light treatment, the photosensitizer is allowed to clear from the body. Because of the short half-life time (0.6 μs) and diffusion distance (0.1 μm) of $^1O_2$ in aqueous media, PDT can be considered a highly selective form of cancer treatment. If the photosensitizer is nontoxic in the absence of light, only the irradiated areas are affected.[20]

An optimized photosensitizer must therefore possess at the same time a large collection of different properties, namely: (i) a sharp and intense absorption band (either one- or two-photon accessible) mainly localized in the biological tissues transparency window (700−900 nm), (ii) good solubility in a biological environment, (iii) an almost absent dark toxicity, (iv) high singlet oxygen sensitization quantum yield, (v) preferential localization within the tumor, and (vi) easy after-treatment removal from the body.

The first-generation photosensitizers, and up to now still the only one approved by FDA for human treatment, are hematoporphyrin derivatives such as Photofrin. Photofrin-mediated PDT has proved successful for a wide range of cancers; nonetheless, a number of drawbacks and side effects are well-documented.[21] This drug being a complex mixture, there are questions concerning the identity of the active components and also about the reproducibility of the synthetic process. The treatment commonly involves the use of laser light at 630 nm. At this wavelength, the laser beam can penetrate the tissue only to a maximum depth of 3−10 mm, clearly limiting the therapy applicability to superficial diseases. After treatment, light sensitization can last for several weeks and patients are advised to avoid bright light during this period. Because of all of these drawbacks, new photosensitizers have been synthesized. The so-called second-generation photosensitizers mainly include modified porphyrins (protoporphyrin IX and its precursor aminolevulinic acid among them),[22] chlorines, bacteriochlorins, texaphyrines, phthalocyanines, naphthalocyanines, pheophorbides, purpurins, and squaraines.[23]

Ogilby and co-workers have recently shown that $^1O_2$ can also be produced and optically detected upon two-photon nonlinear excitation of the sensitizer with a focused laser beam.[24] The two main advantages of such a technique are the intrinsic 3D resolution of the two-photon absorption (TPA)-prompted excitation processes, already widely exploited for example in fluorescence imaging[25] and microfabrication,[26] and the use of NIR sources, with a consequent increase in the light penetration depth.

Some of us recently reported the design and synthesis of π-extended squaraines displaying an exceedingly strong TPA efficiency with cross sections nearly 1 order of magnitude higher than that of the majority of the compounds previously reported.[27] We also communicated on their possible use as one-photon $^1O_2$ sensitizers pertinent to PDT.[28] Because of the constitutional flexibility of some of the compounds we made, we felt it was important to further investigate more specifically and on the whole the behavior of heterocycle-based π-extended squaraines to get further insight into the synthetic design strategies required to get at the same time a strong TPA behavior and fulfill the many demanding requirement of modern PDT sensitizers.[29]

When looking at π-extended squaraines as a possible new class of TPA active photosensitizers, we also focused, in view of a possible clinical application, on the optimization of the TPA behavior in a region close to 800 nm, the fundamental output of standard commercially available femtosecond Ti:sapphire laser sources.

We report herein the synthesis, electrochemical, linear, and nonlinear optical characterization as well as evidence for singlet oxygen sensitization, toxicity studies, and in vitro cellular staining capabilities of selected members of three classes of new

(12) (a) Bonnett, R. *Chemical Aspects of Photodynamic Therapy;* Gordon and Breach Science: Amsterdam, 2000. (b) Pushpan, S. K.; Venkatraman, S.; Anand, V. G.; Sankar, J.; Parmeswaran, D.; Ganesan, S.; Chandrashekar, T. K. *Curr. Med. Chem.: Anti-Cancer Agents* **2002**, *2*, 187. (c) Allison, R. R.; Downie, G. H.; Cuenca, R.; Hu, X.-H.; Childs, C. J. H.; Sibata, C. H. *Photodiagn. Photodyn. Ther.* **2004**, *1*, 27. (d) Dolmans, D. E. J. G. J.; Fukumura, D.; Jain, R. K. *Nat. Rev. Cancer* **2003**, *3*, 380.

(13) MacDonald, I. J.; Dougherty, T. J. *J. Porphyrins Phthalocyanines* **2001**, *5*, 105.

(14) Hooper, C. Y.; Guymer, R. H. *Clin. Exp. Ophthalmol.* **2003**, *31*, 376.

(15) (a) Sharman, W. M.; Allen, C. M.; van Lier, J. E. *Drug Discovery Today* **1999**, *4*, 507. (b) Dougherty, T. J.; Gomer, C. J.; Henderson, B. W.; Jori, G.; Kessel, D.; Korbelik, M.; Moan, J.; Peng, Q. *J. Natl. Cancer Inst.* **1998**, *90*, 889. (c) Bonnett, R. *Chem. Soc. Rev.* **1995**, *24*, 19.

(16) (a) Lipson, R. L.; Baldes, E. J.; Olsen, A. M. *J. Natl. Cancer Inst.* **1961**, *26*, 1−11. (b) Brown, S. B.; Truscott, T. G. *Chem. Br.* **1993**, *29*, 955. (c) Dougherty, T. J.; Marcus, S. L. *Eur. J. Cancer* **1992**, *28A*, 1734.

(17) Niamien Konan, Y.; Gurny, R.; Allémann, E. *J. Photochem. Photobiol., B* **2002**, *66*, 89.

(18) (a) Foote, C. S. *Acc. Chem. Res.* **1968**, *1*, 104. (b) *Singlet Oxygen;* Frimer, A. A., Ed.; CRC Press: Boca Raton, FL, 1985; Vols. I−IV. (c) Foote, C. S.; Clennan, E. L. In *Active Oxygen in Chemistry;* Foote, C. S., Valentine, J. S., Greenberg, A., Liebman, J. F., Eds.; Chapman and Hall: London, 1995; pp 105−140. (d) Ogilby, P. R.; Kristiansen, M.; Martire, D. O.; Scurlock, R. D.; Taylor, V. L.; Clough, R. L. *Adv. Chem. Ser.* **1996**, *249*, 113. (e) Wilkinson, F.; Helman, W. P.; Ross, A. B. *J. Phys. Chem. Ref. Data* **1993**, *22*, 113.

(19) Oleinick, N. L.; Morris, R. L.; Belichenko, I. *Photochem. Photobiol. Sci.* **2002**, *1*, 1.

(20) Henderson, B. W.; Dougherty, T. J. *Photochem. Photobiol.* **1992**, *55*, 145.

(21) Ochsner, M. *Drug Res.* **1997**, *47*, 1185.

(22) (a) Peng, Q.; Berg, K.; Moan, J.; Kongshaug, M.; Nesland, J. M. *Photochem. Photobiol.* **1997**, *65*, 235. (b) Dierickx, C. C.; Anderson, R. R. *Int. Photodyn.* **1996**, *1*(4), 2. (c) Marcus, S. L. *Int. Photodyn.* **1996**, *1*(5), 2. (d) Patrice, T. *Int. Photodyn.* **1995**, *1*, 1. (e) Barr, H. *Int. Photodyn.* **1995**, *1*, 6. (f) Barr, H.; Overholt, B. F.; Panjepour, M.; Wang, K. K.; Laukka, M.; Gutta, K. *Int. Photodyn.* **1995**, *1*, 7.

(23) For a recent review, see: Morone, M.; Beverina, L.; Abbotto, A.; Pagani, G. A. *Targets Heterocycl. Syst.* **2005**, *9*, 66.

(24) (a) Frederiksen, P. K.; McIlroy, S. P.; Nielsen, C. B.; Nikolajsen, L.; Skovsen, E.; Jørgensen, M.; Mikkelsen, K. V.; Ogilby, P. R. *J. Am. Chem. Soc.* **2005**, *127*, 255. (b) Arnbjerg, J.; Johnsen, M.; Frederiksen, P. K.; Braslavsky, S. E.; Ogilby, P. R. *J. Phys. Chem. A* **2006**, *110*, 7375. (c) Arnbjerg, J.; Jiménez-Banzo, A.; Paterson, M. J.; Nonell, S.; Borrell, J. I.; Christiansen, O.; Ogilby, P. R. *J. Am. Chem. Soc.* **2007**, *129*, 5188. (d) Frederiksen, P. K.; Jorgensen, M.; Ogilby, P. R. *J. Am. Chem. Soc.* **2001**, *123*, 1215.

(25) (a) Denk, W.; Strickler, J. H.; Webb, W. W. *Science* **1990**, *248*, 73. (b) So, P. T. C.; Dong, C. Y.; Masters, B. R.; Berland, K. M. *Annu. Rev. Biomed. Eng.* **2000**, *2*, 399.

(26) (a) Strickler, J. H.; Webb, W. W. Two-Photon Excitation in Laser Scanning Fluorescence Microscopy. In Proceedings of CAN-AM Eastern '90; Antos, R. L., Krisiloff, A. J., Eds.; SPIE: Rochester, NY, 1990; Proceedings Vol. 1398, pp 107−118. (b) Maruo, S.; Nakamura, O.; Kawata, S. *Opt. Lett.* **1997**, *22*, 132. (c) Cumpston, B. H.; Ananthavel, S. P.; Barlow, S.; Dyer, D. L.; Ehrlich, J. E.; Erskine, L. L.; Heikal, A. A.; Kuebler, S. M.; Lee, I.-Y. S.; McCord-Maughon, D.; Qin, J.; Röckel, H.; Rumi, M.; Wu, X.-L.; Marder, S. R.; Perry, J. W. *Nature* **1999**, *398*, 51.

(27) Chung, S.-J.; et al. *J Am. Chem. Soc.* **2006**, *128*, 14444.

(28) Beverina, L.; Abbotto, A.; Landenna, M.; Cerminara, M.; Tubino, R.; Meinardi, F.; Bradamante, S.; Pagani, G. A. *Org. Lett.* **2005**, *7*, 4257.

(29) Gorman, A.; Killoran, J.; O'Shea, C.; Kenna, T.; Gallagher, W. M.; O'Shea, D. F. *J. Am. Chem. Soc.* **2004**, *126*, 10619.

Scheme 1

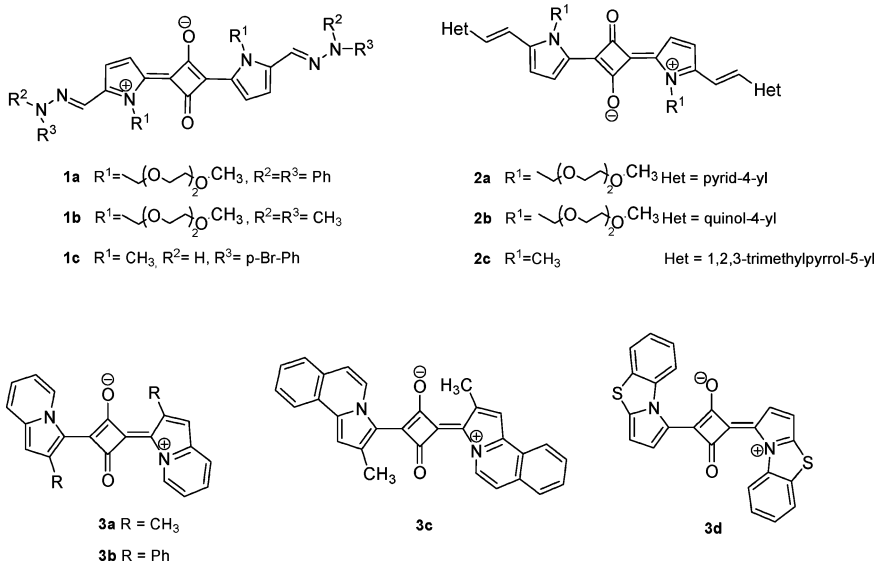

Scheme 2

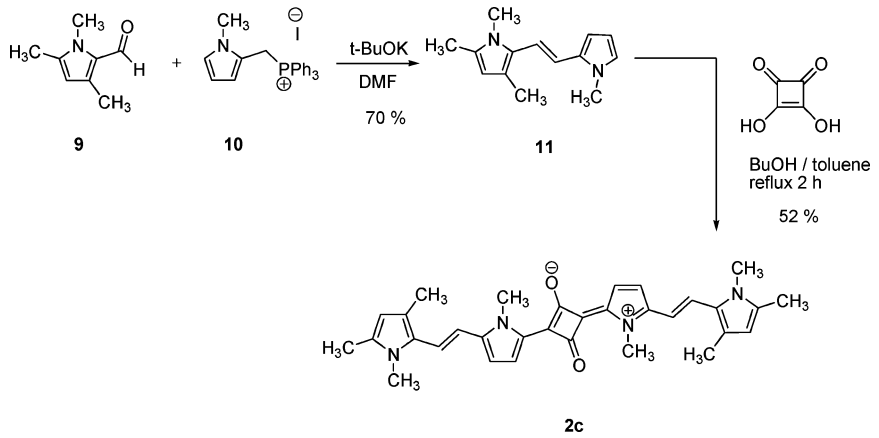

squaraines identified by their different Arabic numbers while letters identify their different substituents or skeletons (Scheme 1).

Results and Discussion

Design and Synthesis of the Squaraines. Derivatives **1a**−**c** and **2a**,**b** were obtained as previously described by refluxing the appropriate arylhydrazonomethylpyrroles or bisheteroarylethane and squaric acid in a BuOH/toluene mixture for 1−3 h.[28]

Although in the previously reported derivatives **2a**,**b** we chose to extend the conjugation length upon the introduction of a mild electron-withdrawing group as an electron-deficient heteroaromatic ring, with the new derivative **2c** we introduced a further mild donor as a second pyrrole ring. Derivative **2c** was thus obtained starting from the bispyrrolylethylene derivative **11** (prepared in good yield under standard Wittig olefination conditions from *N*-methylpyrrole triphenylphosphonium iodide **10** and 1,3,5-trimethylpyrrole-2-carbaldehyde **9** in anhydrous DMF with *t*BuOK as a base) and squaric acid in refluxing BuOH in the presence of toluene as an azeotropic water removal solvent. Product **2c** was found to be an almost insoluble powder and was directly isolated in high yield simply by filtration (Scheme 2).

Concerning class **3** molecules, derivatives **3b**−**d** are new examples of an original squaraine family we recently introduced.[28] With respect to the first term **3a**, we studied two different strategies to increase the conjugation length: (a) the substituent effect in **3b**, and (b) the ring fusion effect in **3c**. Finally, in the case of derivative **3d**, we aimed to study whether a sulfur atom, instead of the widespread employed but not completely biological friendly halogen atoms, could work as a heavy atom in the singlet oxygen sensitization enhancement.[11] In all of the cases, we followed the synthetic strategy involving the reaction of the known preformed indolizine derivative with squaric acid under the standard conditions we chose: refluxing BuOH/toluene (Scheme 3).

Spectroscopic Characterization. One of the prominent targets of second-generation sensitizers for photodynamic therapy is their operational spectral window to be partially or completely included in the tissue transparency region, both as one- and two-photon activated dyes.

Accordingly, in the design of squaraines for PDT, our first concern was the tuning of their optical band gap. We characterized all of the derivatives both in phosphate-buffered saline (PBS) solution and in methylene chloride. Some of the squaraines we made were found to be very soluble in water (derivatives **2a** and **1b** particularly). For the water-insoluble derivatives, we used the nontoxic emulsifier, Cremophor EL (CrEL), frequently used in vivo as the delivery agent for poorly

Scheme 3

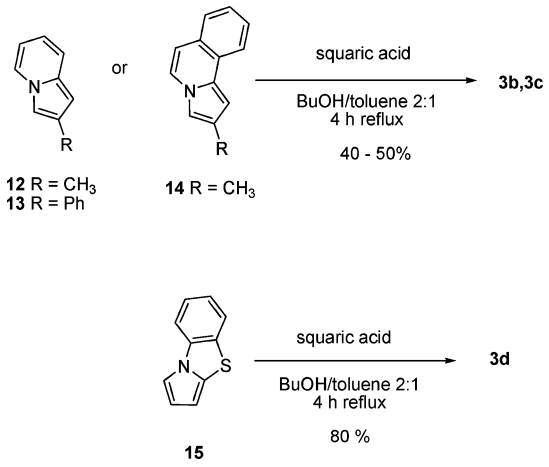

Table 1. Linear Absorption Parameters of Compounds **1**−**3**

compd	λ_{max} CH_2Cl_2 (nm)	λ_{max} form PBS (nm)	absorption cutoff (PBS)	ϵ (mol^{-1} l cm^{-1}) CH_2Cl_2
1a	728	734	815	239 000
1b	688	693	765	252 000
1c	717	745	880	154 000
2a	678	681	775	254 000
2b	688	698	785	260 000
2c	767	779, 691	965	135 000
3a	684	688	820	178 000
3b	698	701	795	135 000
3c	685	not soluble		250 000
3d	636	641	830	142 000

water-soluble anticancer drugs[30] to get water solution of the dyes for spectroscopic characterization.[31]

Table 1 shows the UV−vis absorption characteristics of squaraines **1**−**3** in both CH_2Cl_2-and CrEL-formulated PBS. Their main absorption bands span all over the red NIR region, and peak wavelengths range from 636 to 767 nm, well within the tissue transparency spectral window. The absorption cutoffs are relevant in the TPA characterization. The aim of the present research is the optimization of dyes TPA performances at 806 nm; no chromophore linearly absorbing at this wavelength can be considered for clinical applications.

It is apparent that in the family **1** compounds the S_0-S_1 transition energy variation is mainly associated with the presence of aromatic vs aliphatic substituents on the hydrazonic nitrogen and only marginally by the kind of substituent present on the aromatic ring. In particular, on judging from the cutoff data (defined as the ABS < 0.01 wavelength), only end-capped aliphatic hydrazone derivatives (like **1b**), among all the possible class **1** compounds, appear to be relevant for the present study (Figure 1).

Family **2** squaraines show a more striking dependence of the absorption energy band on the substitution path. In fact, while the ring fusion effect on the electron acceptor moiety we exploited on going from the pyridine end-capped derivative **2a** to the quinoline derivative **2b** only leads to a negligible 27 meV

(30) Gelderblom, H.; Verweij, J.; Nooter, K.; Sparreboom, A. *Eur. J. Cancer* **2001**, *37*, 1590.

(31) The formulation procedure required dissolving the photosensitizer in the minimum quantity of the appropriate organic solvent (often CH_2Cl_2) and treating the solution with a mixture of CrEl and 1,2-propanediol (10:3 v/v). This was sonicated for up to 30 min followed by removal of the volatile solvent under vacuum. The resulting oil was dissolved in PBS solution followed by filtration through a 0.2-mm membrane filter.

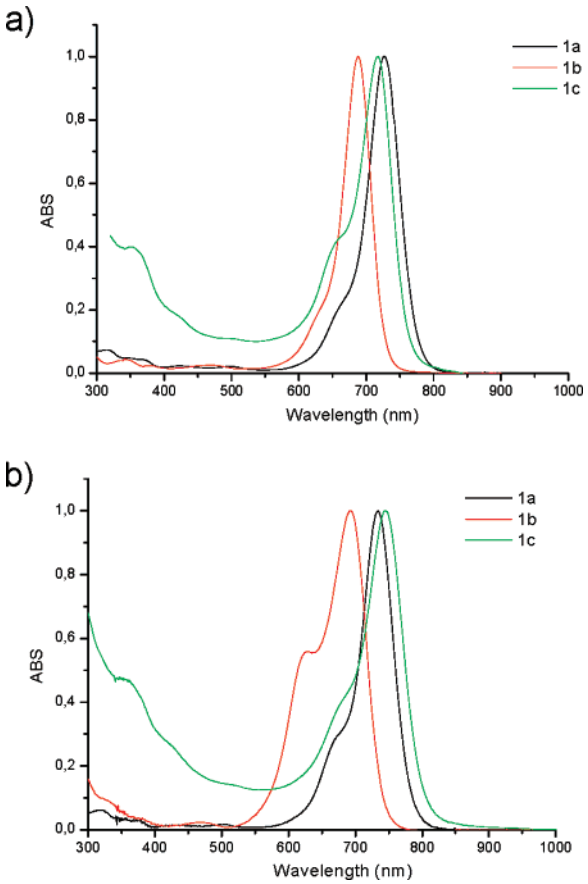

Figure 1. UV−vis absorption spectra of class **1** squaraines in (a) CH_2Cl_2- and (b) CrEL-formulated PBS.

bathochromic shift, the substitution of a mild electron-accepting ring with a donating one, a second pyrrolic unit, results in **2c** in a major red shift of nearly 212 meV. In derivative **2c**, the large red shift goes together with a slight broadening of the whole absorption band. Although an absorption red shift in family **2** compounds was required to optimize TPA performances at 800 nm, the band gap narrowing we obtained with **2c** was too large for the purpose of the present work (Figure 2a).

In the family **3** compounds, we observed a relatively small bathochromic shift on going from the parent compound **3a** to the phenyl-substituted **3b**, in agreement with a conjugation length increase effect. Surprisingly, however, the ring fusion effect we explored on going from **3a** to **3c** did not result in a similar bathochromic shift but only in a slight narrowing of the absorption band.

The case of derivative **3d** is different, the latter in fact is not comparable with the indolizinic derivatives **3a**−**c** but rather with an *N*-phenyl-2-arylthiopyrrole derivative. The conjugation length in **3d** is accordingly significantly reduced with respect to the parent compound **3a**, and hence the observed ipsochromic shift (Figure 3). Unfortunately, although in principle compound **3c** is very attractive on judging from its spectroscopic features, the only 800-nm transparent family **3** derivative was found to be completely water insoluble, even in the presence of large amounts of CrEL.

Electrochemical Characterization. We investigated the electrochemistry of class **1** and **2** squaraines with cyclic voltammetry to evaluate the extension of their conjugation upon

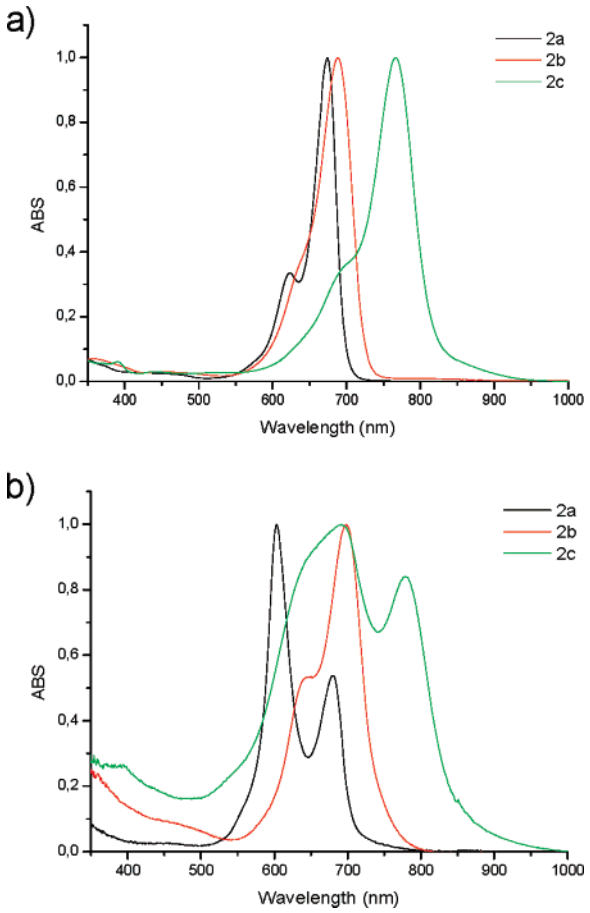

Figure 2. UV−vis absorption spectra of class **2** squaraines in (a) CH_2Cl_2- and (b) CrEL-formulated PBS.

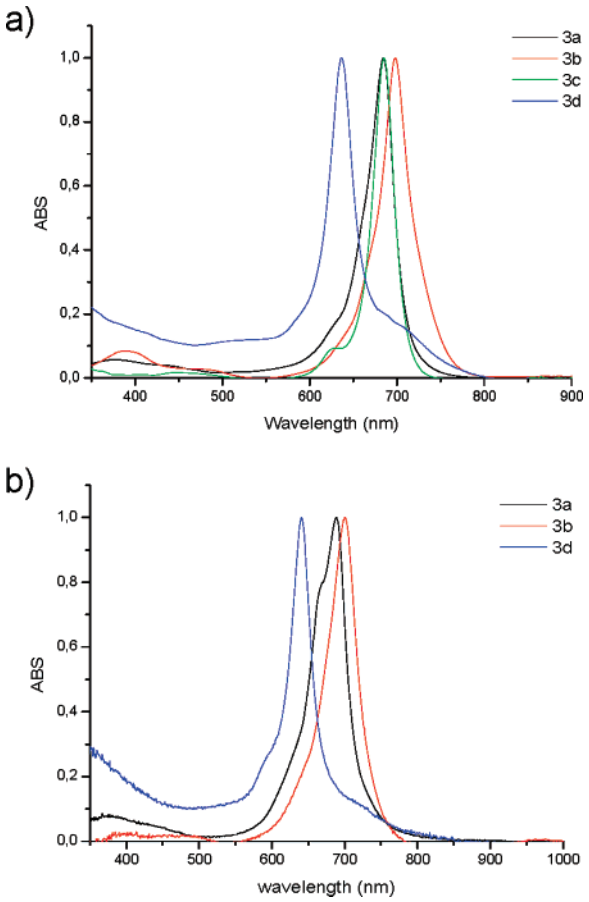

Figure 3. UV−vis absorption spectra of class **3** compounds in (a) CH_2Cl_2- and (b) CrEl-formulated PBS.

Table 2. Half-Wave Potentials ($E_{1/2}$ vs Fc/Fc^+), Peak Separation Values for Each Process for Which an $E_{1/2}$ Value Is Reported (ΔEp) along with the Corresponding Value, in Italic, for Ferrocene (ΔEp_{fc}), Peak Separation between the First and the Second Redox Processes (ΔE), and Cathodic Peak Potentials for Irreversible Reduction (E_{pc}^{red}) of Class **1** and **2** Squaraines in CH_3CN with Tetrabutylammonium *p*-Toluenesulphonate as the Supporting Electrolyte; Values Are in Volts

compd	$E_{1/2}$ (**1**)	ΔEp (1) (ΔEp_{fc})	$E_{1/2}$ (**2**)	ΔEp (2) (ΔEp_{fc})	ΔE	E_{pc}^{red}
1a	0.18	0.065 (*0.062*)	0.46	0.060 (*0.062*)	0.28	−1.10
1b	−0.06	0.073 (*0.072*)	0.19	0.085 (*0.072*)	0.25	−1.06
2a	−1.19					
2b	−1.21					
2c	−0.19	0.080 (*0.064*)	−0.11	0.085 (*0.064*)	0.08	−1.35

introducing either electron-rich (**1a**−**c**, **2c**) or electron-poor (**2a**, **2b**) end-capping groups. On doing this, we also aimed to characterize the redox processes in π-extended squaraines in general.[32] In all of the symmetric derivatives we described, if the two identical end-capping groups are redox active, they can be either weakly or strongly coupled, according to the efficiency of the conjugation along the chromophore backbone. If the two centers are coupled, we expect to observe two one-electron processes with a peak potential separation. Although this peak separation cannot be considered a quantitative gauge for the coupling strength, it can be used as a qualitative tool for the conjugation efficiency ranking.[33]

The cyclic voltammograms (CV) for all of the family **1** and **2** derivatives are reported in the Supporting Information. Table 2 shows the half-wave potentials ($E_{1/2}$ vs Fc/Fc^+), peak separation between the first and the second redox process (ΔE), and half-wave potentials for irreversible reduction ($E_{1/2}^{red}$) of class **1** and **2** squaraines in CH_3CN with tetrabutylammonium *p*-toluenesulphonate as the supporting electrolyte.

Squaraine **1a** CV plot displays two reversible redox waves at positive potentials (oxidizing) and one irreversible wave at negative (reducing) potentials (Figure SI2 of the Supporting Information). We interpret the two positive potential waves as the oxidations of the two hydrazonic moieties and the negative potential wave as the irreversible reduction of the electron-poor squaraine core. The large potential shift between the two waves is evidence for a strong electron coupling between the two hydrazone units, a feature no doubt associated with the very efficient conjugation along the whole molecular structure.

The introduction of an alkyl substituent on the hydrazonic nitrogen on going from **1a** to **1b** results in a remarkable decrease of the oxidation potential, together with a decrease in the potential shift between the two reversible waves (Figure SI3 of the Supporting Information). It has been reported that, in the case of aniline-based squaraines, the substituents both at the nitrogen atom and in the phenyl ring have a strong influence on the oxidation potential, which decreases on increasing the electron-donating ability of the substituent.[34] The drop in the oxidation potential is also plausibly the cause for the general lower stability to oxidative stress of molecule **1b** with respect

(32) Bulschel, M.; Ajayaghosh, A.; Arunkumar, E.; Daub, J. *Org. Lett.* **2003**, *5*, 2975.
(33) Barriere, F.; Camire, N.; Geiger, W. E.; Mueller-Westerhoff, U. T.; Sanders, R. *J. Am. Chem. Soc.* **2002**, *124*, 7262.

Scheme 4

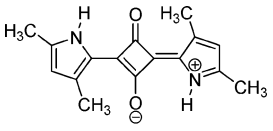

16

to **1a** in the collisional quenching $^1O_2$ sensitization measurements we previously reported.[28]

The CV plot of class **2** molecules is of no particular significance for derivatives **2a** and **2b**, where no oxidizable group is present (Figures SI4 and SI5 of the Supporting Information, respectively). In the case of derivative **2c**, the presence of the second pyrrole unit gives rise to three partially reversible oxidation waves at −0.19, −0.11, and 0.20 eV versus Fc/Fc^+. Squaraine **2c** possesses the highest HOMO in the series. The presence of a third oxidation wave, although unexpected, could be associated with the oxidation of the pyrrole ring directly connected with the squaraine core. We have no evidence of squaraine degradation during the measurement (Figure SI6).

Two-Photon Absorption Measurements. The TPA cross sections σ of molecules **1a**, **1b**, and **2b** together with the model pyrrole squaraine **16** (Scheme 4) investigated for comparison were measured in DMSO by open aperture Z-scan[35] experiments at 806 nm using ∼150-fs-long pulses.

Examples of Z-scan plots for derivatives **1b** and **2b** are shown in Figure 4 in the upper and lower panels, respectively. The concentration used to record the Z-scan trace of compound **16** is more than 1 order of magnitude higher than that for all other compounds, evidence for a very small optical nonlinearity of **16** at the employed wavelength.

Compound **1a** was previously characterized using the same technique in a different solvent: THF and in the wavelength range 825−1080 nm.[27] Indeed, at 806 nm **1a** has already a perceptible linear absorption. Its signal is strongly affected by multiphoton absorption phenomena involving direct population of the first excited state, as can be noticed from the Z-scan trace in Figure 5. In contrast with the previous Z-scan traces, the normalized transmittance of sample **1a** increases as the laser fluence increases, showing a maximum at the focal position. This behavior can be attributed to saturation phenomena of the one-photon transition at 806 nm.

As discussed in the Supporting Information, the TPA coefficient σ of molecules **1b** and **2b** was measured as a function of input laser fluence at the focal plane. Results are depicted in Figure 6.

The marked decrease of the TPA cross section for both compounds as the laser fluence increases is a clear sign that the observed nonlinear absorption is not a simple third-order coherent TPA process but a higher order multiphoton absorption process, involving excited-state transitions different from the two-photon allowed one. To fully understand the physical origin of this behavior, further photophysical characterizations are necessary. Table 3 summarizes the TPA cross sections for the investigated compounds. In particular, for **1b** and **2b**, σ is given as (i) an average value calculated on all the data recorded, irrespective of laser fluence employed, and (ii) a limiting value at zero fluence. The latter has been extrapolated from a linear fit of the data shown in Figure 6.

To make a quantitative comparison of the different squaraine performances, it would be necessary to record the whole TPA spectrum. In the present article, however, we were not interested

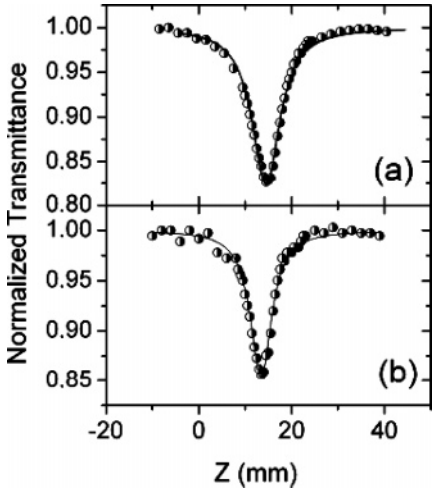

Figure 4. Z-scan experimental data (a) of compound **1b** in DMSO (2.4×10^{-4} M) (circles) and (b) of compound **2b** in DMSO (1.3×10^{-4} M) (circles) in a 1-mm cell. Solid lines are the result of a fit to the data points.

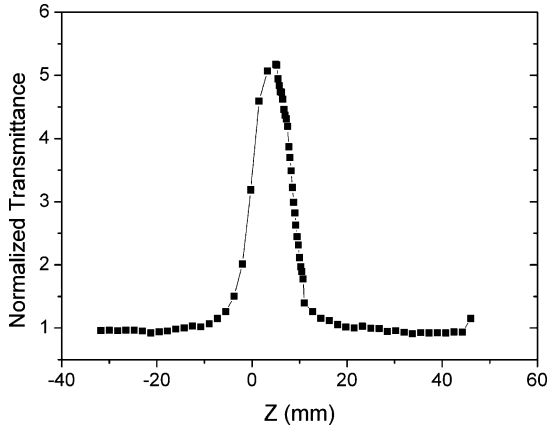

Figure 5. Z-scan experimental data of compound **1a** in DMSO (1.0×10^{-3} M) in a 1-mm cell. Full line is just a guide to the eye.

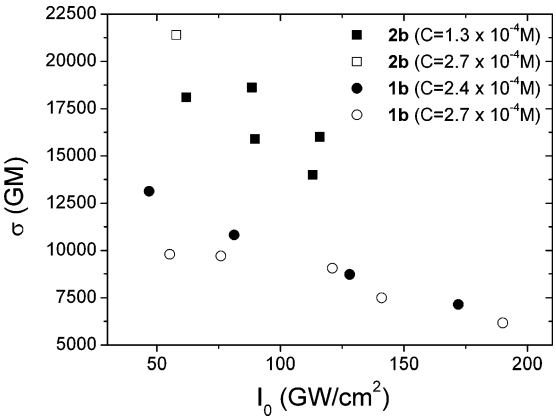

Figure 6. Value of the TPA cross section of **1b** and **2b** in DMSO measured as a function of the input laser fluence at the focal plane.

(34) Law, K.-Y.; Facci, J. S.; Balley, F. C.; Janus, J. F. *J. Imaging Sci.* **1990**, *34*, 31.
(35) (a) Sheik-Bahae, M.; Said, A. A.; Wei, T.-H.; Hagan, D. J.; Van Stryland, E. W. *IEEE J. Quantum Electron.* **1990**, *26*, 760. (b) Wei, T. H.; Hagan, D. J.; Sense, M. J.; Van Stryland, E. W.; Perry, J. W.; Coulter, D. R. *Appl. Phys. B* **1992**, *54*, 46.

Table 3. TPA Cross Section Coefficients of Compounds **1a**,**b**, **2b**, and **16** (DMSO)

compd	$\langle\sigma\rangle^a$ (GM)^c	$\sigma\ (I_0 = 0)^b$ (GM)^c
1b	9100 ± 2000	13 300 ± 800
2b	17400 ± 2400	24 000 ± 2000
1a	N.D. (linear absorption)	
16	18 ± 10	

[a] Average value of the TPA cross section calculated from all the data recorded, irrespective of laser fluence. [b] Average value of the TPA cross section calculated from a linear fit of the measured data at zero laser fluence. [c] 1 GM (Göppert-Mayer) = 1×10^{-50} cm^4 s photon^{-1} molecule^{-1}.

Table 4. Results of the One-Photon Sensitization Measurements for Squaraine **1a**, **1b**, and **2b** with Respect to Two Different Standards: *meso*-TPP and 2CA

compd	$^1O_2$ quantum yield[a]	$^1O_2$ quantum yield[b]
1a	0.16 ± 0.04	0.17 ± 0.04
1b	0.025 ± 0.007	0.025 ± 0.009
2b	0.33 ± 0.06	0.35 ± 0.08
meso-TPP	0.51	
2CA		2

[a] Calculated using *meso*-TPP as standard. [b] Calculated using 2CA as standard.

in TPA structure−property relationships but rather in the characterization of the photosensitizer behavior at a wavelength that is becoming readily available for biomedical applications. The single wavelength σ values we obtained are fairly large, ranking squaraines **1b** and **2b** among the state of the art two photon dyes.

One- and Two-Photon Absorption-Induced Singlet Oxygen Generation. The net performance of a TPA photosensitizer can be estimated as the product of its linear $^1O_2$ quantum yield and of its TPA cross section. To better understand the overall squaraine performance, we chose first to independently measure the linear $^1O_2$ quantum yield and then to perform the two-photon excitation experiment.

One-Photon Sensitization Measurements. The one-photon $^1O_2$ generation performances of class **1** and **2** molecules was previously investigated using the collisional quenching method.[28] By means of this indirect method, we were able to qualitatively estimate derivatives **1** and **2** efficiencies to be about 10% of that of *meso*-tetraphenylporphyrin (*meso*-TPP), the reference compound for PDT sensitizers.[36] We have now performed a direct measurement involving the observation of the dye-sensitized singlet oxygen phosphorescence emission at 1270 nm.

For the one-photon experiments, we chose two different standards: *meso*-TPP and 9,10-dichloroanthracene (2CA),[37] both possessing a good $^1O_2$ sensitization yield. We chose CS_2 as the solvent for the sensitization measurements because of the good solubility of all the compounds and standards in this solvent and because of the high radiative efficiency of $^1O_2$, enabling easy detection of the phosphorescence signal. The investigation was carried out on derivatives **1a** and **1b**, whose activities were expected to be strongly different, and on derivative **2b** as a representative of family **2** compounds.[38] Table 4 summarizes the results of the one-photon sensitization measurements. The two different standards gave comparable results.

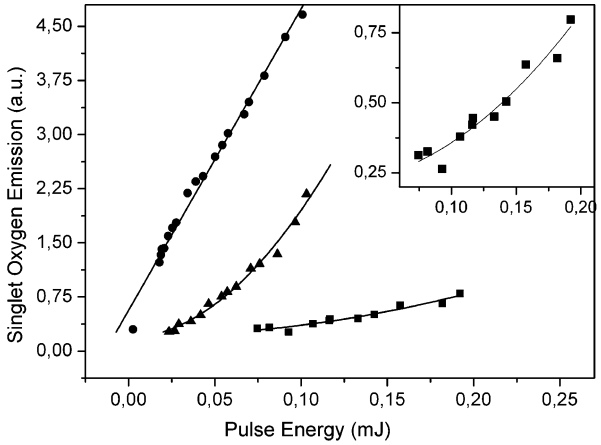

Figure 7. $^1O_2$ phosphorescence signal at 1270 nm, recorded upon two-photon excitation at 806 nm, of the CS_2 solution of squaraines **1a** (●), **1b** (■), and **2b** (▲) as a function of the energy of the applied laser pulses. The inset shows an enlargement for the **1b** data.

It is commonly accepted that a good sensitizer for one-photon absorption-prompted PDT should display an $^1O_2$ quantum yield of at least 0.3 to suit the requirements of practical applications such as exposure time and total irradiation dose. This criterion is satisfied only by compound **2b**. Although **1a** and **2b** squaraines show only moderate sensitization efficiencies, their TPA cross sections are almost 4 orders of magnitude higher than those of all other reported NIR singlet oxygen sensitizers, and in particular of *meso*-TPP and the structurally related, commonly employed, hematoporphyrines such as Photofrin.[39]

Two-Photon Sensitization Measurements. The TPA $^1O_2$ generation experiment was carried out under the same experimental conditions described for direct excitation, but in this case employing the 806-nm output of the amplified Ti:sapphire femtosecond laser at the repetition rate of 200 Hz. The two reference standards, *meso*-TPP and 2CA, do not give any detectable signal when pumped at 806 nm, while all of the compounds **1a**, **1b**, and **2b** show $^1O_2$ phosphorescence.

Figure 7 shows the dependence of the $^1O_2$ phosphorescence signal for the CS_2 solution of squaraines **1a**, **1b**, and **2b** as a function of the energy of the applied laser pulses. The full lines are the result of a quadratic fit for **1b** and **2b** and of a linear fit for **1a**. An enlargement of the data for **1b** is displayed in the inset. For this data set, the quadratic dependence was confirmed by fitting the data with a power law whose exponent turned out to be 2.04. The anticipated extremely intense signal we measured for derivative **1a**, together with its linear dependence with respect to the energy of the applied pulses, is a consequence of a weak linear absorption of this squaraine at the employed wavelength. The quadratic behavior observed for the $^1O_2$ emission of **1b** and **2b** is a clear sign of the TPA nature of the process giving rise to $^1O_2$ production by these two molecular compounds.

Table 5 shows the TPA cross section and $^1O_2$ quantum yields of selected TPA photosensitizers among the various ones that have been proposed in the literature, in comparison with **1b** and **2b** performances. In particular, BrPhVB is 4-(4-(4-(dimethylamino)styryl)-2,5-dibromostyryl)-*N*,*N*-dimethylbenzenamine and is often considered a standard for both TPA and

(36) Gollnick, K.; Griesbeck, A. *Tetrahedron* **1985**, *41*, 2057.
(37) Wilkinson, F.; Helman, W. P.; Ross, A. B. *J. Phys. Chem. Ref. Data* **1993**, *22*, 113.
(38) **2a** and **2b** efficiencies were expected to be comparable from our previous experience, and compound **2a** is not soluble in CS_2 and only sparingly soluble in other common organic solvents.
(39) Morone, M.; Beverina, L.; Abbotto, A.; Silvestri, F.; Collini, E.; Ferrante, C.; Bozio, R.; Pagani, G. A. *Org. Lett.* **2006**, *8*, 2719 and references therein.

Table 5. σ_{TPA} and $^1O_2$ Quantum Yield ϕ Values for Selected TPA Sensitizers Known in the Literature; the σ_{TPA} ϕ Product Is Reported as the Figure of Merit for the Net Chromophore Efficiency

compd	TPA cross section (GM)	$^1O_2$ quantum yield ϕ	net chromophore efficiency $\sigma\phi$
meso-TPP[39]	16[a]	0.51[d]	8
BrPhVB[24b]	460[b]	0.37[b]	170
TPPo[24c]	2280[c]	0.23[c]	524
PdTPPo[24c]	1750[c]	0.78[c]	1365
1b	9100[a]	0.03[d]	273
2b	17400[a]	0.33[d]	5742

[a] DMSO @ 806 nm, femtosecond excitation source Ti:sapphire. [b] Cyclohexane @ 800 nm, femtosecond excitation source Ti:sapphire. [c] Toluene @ 770 nm, femtosecond excitation source Ti:sapphire. [d] CS_2.

singlet oxygen generation, whereas TPPo and PdTPPo are tetraphenylporphycene and its palladium complex, respectively. TPPo and PdTPPo rank among the most performing dyes ever reported for TPA PDT.[24c] In the end, even if squaraine intrinsic sensitization properties are only modest, the combination with their exceedingly strong TPA makes them comparable with the state of the art.

Cellular Localization. Derivatives **1b** and **2a** possess, in contrast to the vast majority of the known PDT photosensitizers, a remarkably high water solubility. It was accordingly possible to directly employ PBS water solution of the dyes without the use of any solubilizing agent such as CrEL. In the preparation of the dye solution before cell incubation, we became aware of a severe aggregation behavior in the employed buffer solution and in water in general. In fact, just to cite an example, while the EtOH and CrEL-formulated water solutions of derivative **2a** do not show any remarkable change in the peak position or in the bandwidth at half the maximum, the PBS solution absorption spectrum shows the uprising of a completely different, strongly blue-shifted band, whose intensity was found to be concentration-dependent.[40] We assigned the new band to the formation of a H-type aggregate, a phenomenon already observed and studied in the case of sandwichlike aggregates of squaraines in water.[41] Our observation suggests that in a biological environment aggregation plays a strong role on the photosensitizer optical properties. This phenomenon is in general only marginally evidenced in CrEL-formulated water solution of water-insoluble derivatives (Figure 8). We submitted derivatives **1b** and **2a** to the toxicity assay based on 3-(4,5-dimethylthiazol-2-yl)-2,5-diphenyltetrazolium bromide on U937 (human leukemic monocyte lymphoma cell line) and human umbilical vein derived endothelial cells (HUVEC), and we did not observe any dark toxicity effect. The cell cultures were then studied by means of a confocal fluorescence microscope enabling for 3D culture resolution.[42] In the case of derivative **1b**, we observed a rapid uptake of the dye, together with an evident localization into extranuclear organelles including

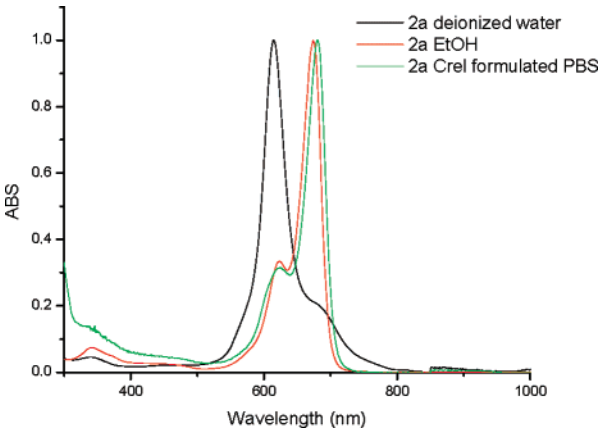

Figure 8. UV−vis absorption spectra of derivative **2a** in deionized water, EtOH, and CrEL-formulated PBS water solution.

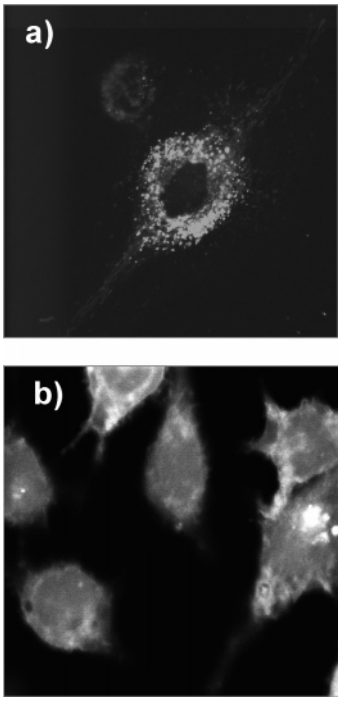

Figure 9. Fluorescence images of cellular localization of (a) derivative **1b** and (b) derivative **2a** in HUVEC. Cells were incubated with a 2 μM solution for 30 min.

mitochondria. In the case of derivative **2a**, we again observed a rapid uptake of the dye, but almost no specific localization into the cell (Figure 9).

Another valuable characteristic of squaraines **1b** and **2a** is their relatively low stability in water solution. We tested the chemical stability of derivative **2a** both in deionized water and in the cell culture medium with comparable results. Figure 10 shows the intensity at the maximum of absorption (in this case, the maximum of the dominating H-aggregate absorption @ 615 nm) as a function of time for a deionized water solution of derivative **2a**. The solution was kept in the dark and at room temperature for nearly 1 day. The total absorption loss is around 20%, and we did not observe the formation of any other colored material. The observed degradation is likely due to hydrolysis, and we further observed very rapid degradation (in the order of seconds) when small amounts of NaOH were added to the

(40) The CrEl-formulated solution was prepared in this case with twice the amount of the emulsifier with respect to the spectrum reported in Figure 2b. This was done to completely suppress the H aggregate. The copresence of the single molecule band and H-aggregate band are anyway already evident from the **2a** spectrum in the formulated PBS we reported in Figure 2b. If no CrEl is added, the only observable absorption pertains to the H-aggregate.

(41) (a) Arunkumar, E.; Ajayaghosh, A.; Daub, J. *J. Am. Chem. Soc.* **2005**, *127*, 3156. (b) Ajayaghosh, A. *Acc. Chem. Res.* **2005**, *38*, 449. (c) Ajayaghosh, A.; Arunkumar, E. *Org. Lett.* **2005**, *7*, 3135.

(42) Dye fluorescence was excited with the 488-nm argon laser line and detected through a long-pass filter above 600 nm by the fast photon-counting mode of the MRC-600 microscope.

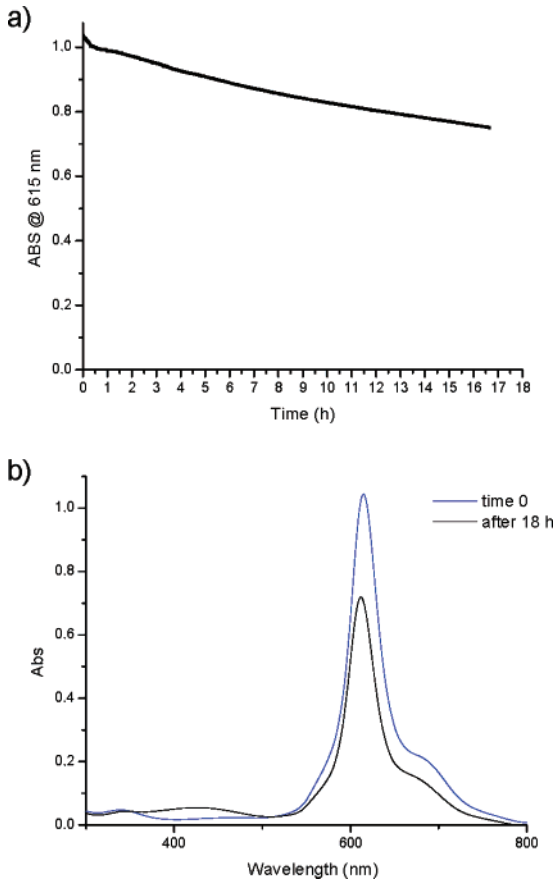

Figure 10. (a) Intensity at the maximum of absorption as a function of time for a deionized water solution of derivative **2a**. (b) Absorption spectra of a freshly prepared and 18 h aged water solution of derivative **2a**.

solution. It has been recently shown, through an ingenious rotaxane-like approach, that the degradation effect is a consequence of the squaric core double bond, highly reactive toward nucleophiles. In fact, in the case of rotaxane-encapsulated squaraine, the dye water stability is greatly enhanced.[9]

The trend we observed in Figure 10 ensures that, in the case of our squaraine photosensitizers, the complete dye clearing from the body, or in any case its deactivation/decomposition, can be sufficiently rapid.

Conclusions

We have described the design criteria, synthesis, and complete characterization of several pyrrole-containing, highly conjugated squaraines appropriate as second-generation photosensitizers for photodynamic therapy. The most performing derivatives we obtained combine an exceedingly strong TPA cross section at 806 nm, the most readily available femtosecond laser source for biomedical applications, and a sizable $^1O_2$ generation efficiency. In contrast with the majority of the previously described second-generation sensitizers, some of the compounds we made are water soluble. These derivatives were characterized in terms of their dark toxicity, cellular uptake, and subcellular localization tendency. We found that derivatives **2a** and **1b** possess sizable fluorescence, enabling for confocal microscopy investigation, together with almost no dark toxicity. Both derivatives were able to efficiently stain HUVEC cells. We provide evidence for a squaraine degradation time, in water solution, of roughly a week, thus enabling for the ready after-treatment photosensitizer deactivation.

In conclusion, because of their very high TPA efficiencies, sizable $^1O_2$ generation performances, almost no dark toxicity, high water solubility, and cellular staining capabilities, selected members among the described structures have potential as photosensitizers for two-photon photodynamic therapy.

Acknowledgment. We thank Ministero Istruzione, Università e Ricerca for financial support of this research (PNR-FIRB RBNE01P4JF and PNR-FIRB RBNE033KMA). Dr. Simone Mazzucato is gratefully acknowledged for his technical help.

Supporting Information Available: Synthetic details for all of the unknown compounds. Technical details on the TPA cross section and singlet oxygen emission experiments. Cyclic voltammetry for compounds **1a**, **1b**, **2a**, **2b**, and **2c**. Complete ref 27. This material is available free of charge via the Internet at http://pubs.acs.org.

JA075933A